Ternary Kv4.2 channels recapitulate voltage-dependent inactivation kinetics of A-type K^+ channels in cerebellar granule neurons

Yimy Amarillo[1], Jose A. De Santiago-Castillo[2], Kevin Dougherty[2], Jonathon Maffie[1], Elaine Kwon[1], Manuel Covarrubias[2] and Bernardo Rudy[1]

[1]*Department of Physiology & Neuroscience and Department of Biochemistry, Smilow Neuroscience Program, New York University School of Medicine, Smilow Research Center, 522 First Avenue, 6th Floor, New York, NY 10016, USA*
[2]*Department of Pathology, Anatomy and Cell Biology, Jefferson Medical College of Thomas Jefferson University, 1020 Locust Street, Philadelphia, PA 19107, USA*

Kv4 channels mediate most of the somatodendritic subthreshold operating A-type current (I_{SA}) in neurons. This current plays essential roles in the regulation of spike timing, repetitive firing, dendritic integration and plasticity. Neuronal Kv4 channels are thought to be ternary complexes of Kv4 pore-forming subunits and two types of accessory proteins, Kv channel interacting proteins (KChIPs) and the dipeptidyl-peptidase-like proteins (DPPLs) DPPX (DPP6) and DPP10. In heterologous cells, ternary Kv4 channels exhibit inactivation that slows down with increasing depolarization. Here, we compared the voltage dependence of the inactivation rate of channels expressed in heterologous mammalian cells by Kv4.2 proteins with that of channels containing Kv4.2 and KChIP1, Kv4.2 and DPPX-S, or Kv4.2, KChIP1 and DPPX-S, and found that the relation between inactivation rate and membrane potential is distinct for these four conditions. Moreover, recordings from native neurons showed that the inactivation kinetics of the I_{SA} in cerebellar granule neurons has voltage dependence that is remarkably similar to that of ternary Kv4 channels containing KChIP1 and DPPX-S proteins in heterologous cells. The fact that this complex and unique behaviour (among A-type K^+ currents) is observed in both the native current and the current expressed in heterologous cells by the ternary complex containing Kv4, DPPX and KChIP proteins supports the hypothesis that somatically recorded native Kv4 channels in neurons include both types of accessory protein. Furthermore, quantitative global kinetic modelling showed that preferential closed-state inactivation and a weakly voltage-dependent opening step can explain the slowing of the inactivation rate with increasing depolarization. Therefore, it is likely that preferential closed-state inactivation is the physiological mechanism that regulates the activity of both ternary Kv4 channel complexes and native I_{SA}-mediating channels.

(Resubmitted 26 December 2007; accepted after revision 12 February 2008; first published online 14 February 2008)
Corresponding author B. Rudy: Smilow Neuroscience Program, Smilow Research Center, New York University School of Medicine, 522 First Avenue, 6th Floor, New York, NY 10016, USA. Email: rudyb01@med.nyu.edu

K^+ channels containing Kv4 pore-forming subunits (Kv4 channels) mediate most of the subthreshold-operating somatodendritic transient or A-type K^+ current in neurons (also known as I_{SA}) (Serodio *et al.* 1994; reviewed in Jerng *et al.* 2004*a*). This current is fundamental to neuronal function. It can contribute to spike repolarization and has critical roles in the modulation of the frequency of repetitive firing, signal processing in dendrites and spike timing-dependent plasticity (Connor & Stevens, 1971; Hoffman *et al.* 1997; Schoppa & Westbrook, 1999; Adams *et al.* 2000; Johnston *et al.* 2000, 2003; Hille, 2001; Liss *et al.* 2001; Ramakers & Storm, 2002; Kim *et al.* 2005, 2007; Chen *et al.* 2006; Hu *et al.* 2006; Thompson, 2007). These functions rely on the precise voltage dependence and kinetic properties of the underlying K^+ channels.

Studies in heterologous expression systems have shown that Kv4 channels may exist as ternary complexes composed of a pore-forming subunit and at least two distinct auxiliary subunits: Kv channel interacting proteins (KChIPs) and the dipeptidyl-peptidase-like proteins (DPPLs) DPPX and DPP10 (An *et al.* 2000; Nadal *et al.*

This paper has online supplemental material.

 DOI: 10.1113/jphysiol.2007.150540

2001, 2003; Jerng *et al.* 2004*b*, 2005; Ren *et al.* 2005; Zagha *et al.* 2005). These associations control the trafficking of channel complexes to the plasma membrane and have major effects on the voltage dependence and kinetics of the channels. However, the significance of these auxiliary proteins in governing the patterns of expression and functional properties of the native I_{SA} channels in neurons has yet to be demonstrated.

The kinetics of inactivation of ternary Kv4 channels expressed in heterologous expression systems has unusual voltage dependence (G. Wang *et al.* 2005; Jerng *et al.* 2007). With increasing step depolarizations, the rate of inactivation slows down. This trend is apparent over a wide range of membrane potentials (−20 to +100 mV; G. Wang *et al.* 2005) and is also observed with binary combinations of Kv4.3 and KChIP1 (Kaulin *et al.* 2008). In contrast, Kv4 channels expressed in the absence of the auxiliary proteins (Serodio *et al.* 1996; Jerng & Covarrubias, 1997; Franqueza *et al.* 1999; Bahring *et al.* 2001; Beck & Covarrubias, 2001; G. Wang *et al.* 2005; S. Wang *et al.* 2005) as well as inactivating channels from other Kv subfamilies (Tseng-Crank *et al.* 1990; Rudy *et al.* 1991; Schroter *et al.* 1991; Vega-Saenz de Miera *et al.* 1992; Riazanski *et al.* 2001) do not exhibit such a voltage dependence.

This unusual behaviour is potentially significant because it has been observed to one degree or another in recordings of A-type K^+ currents from hippocampal neurons (Klee *et al.* 1995; Hoffman *et al.* 1997; Martina *et al.* 1998; Lien *et al.* 2002); however, it has not received much attention and its mechanism is not well understood. Moreover, the I_{SA} is usually only one of several components of the total current observed in whole cell neuronal recordings. Therefore, the I_{SA} has to be properly isolated from other current components to determine its properties accurately. For example, the inactivating current in CA1 hippocampal pyramidal neurons appears to include a contribution from channels that are not members of the Kv4 subfamily (and are possibly mediated by Kv1 subunits) (Chen *et al.* 2006). This is a minor component of the total inactivating current. However, since it has a different voltage dependence and kinetics than the Kv4 component, it would influence the properties of the total inactivating current differently at different membrane potentials.

Previously, we proposed that the unusual voltage dependence of inactivation kinetics is a hallmark of preferential closed-state inactivation in Kv4 channel complexes, and is determined by auxiliary subunits (Kaulin *et al.* 2008). Therefore, this behaviour in neuronal Kv4 channels would suggest that they include a specific combination of Kv4 auxiliary subunits, which confer preferential closed-state inactivation. To test this hypothesis systematically and under stringent conditions, we recorded the I_{SA} from cerebellar granule cells in acute slices and compared the voltage dependence of inactivation kinetics with that of Kv4 channels heterologously expressed in mammalian cells. The latter experiments included the Kv4.2 subunit alone and in binary or ternary complexes with the accessory proteins KChIP1 and DPPX-S. Our results show that the kinetics of inactivation of the I_{SA} in cerebellar granule neurons has a voltage dependence that is remarkably similar to that observed for ternary Kv4 channels containing KChIP and DPPX proteins in heterologous cells. These results support the view that KChIP and DPPX auxiliary proteins are components of the native I_{SA} channels. Furthermore, using kinetic modelling we show that preferential closed-state inactivation and a weakly voltage-dependent opening step can explain the slowing of the inactivation rate with increasing depolarization.

Methods

Electrophysiological recording from heterologous mammalian cells

Electrophysiological recording from heterologous mammalian cells was carried out as previously described (Dougherty & Covarrubias, 2006). Briefly, tsA-201 cells (provided by Dr R. Horn, Thomas Jefferson University, Philadelphia, PA, USA) were transfected with the appropriate plasmids (Kv4.2, KChIP1 and/or DPPX-S) at a 1 : 1 mass ratio using the calcium phosphate method. A plasmid containing a CD8 cDNA (5 μg) was included in the cotransfection to allow the identification of individual transfected cells by decorating them with beads bearing anti-CD8 antibody (Dynal Biotech, Brown Deer, WI, USA) (Kaulin *et al.* 2008). Kv4.2 currents were recorded using the tight-seal whole-cell configuration of the patch-clamp method with a pipette (intracellular) solution containing (mM): 120 KF, 1 $CaCl_2$, 2 $MgCl_2$, 11 EGTA and 10 Hepes, pH 7.2, adjusted with KOH; and the external bath solution containing (mM): 130 NaCl, 2 KCl, 1.5 $CaCl_2$, 1 $MgCl_2$, 20 TEA (tetraethylammonium chloride) and 10 Hepes, pH 7.4, adjusted with NaOH. The calculated free $[Ca^{2+}]$ and $[Mg^{2+}]$ in the intracellular solution were ∼40 nM and ∼1.4 mM, respectively (MaxChelator, WEBMAXC v2.10; http://www.stanford.edu/∼cpatton/maxc.html). Extracellular TEA was necessary to eliminate a small but significant endogenous delayed-rectifier K^+ current. The experiment began once current kinetics and amplitude became stable. Series resistance ($R_s = 2$–5 MΩ) was compensated to yield a total voltage error of < 3 mV. A $P/-4$ leak subtraction protocol consisting of four subpulses from a subsweep holding potential of −110 mV was used to subtract passive components of the total current. Currents were filtered at 2 kHz and sampled at 10 kHz. Analyses and graphical displays were produced with pCLAMP 9.0 (Axon Instruments, Inc., Union City, CA, USA) and Origin 7.5 (OriginLab Corp., Northhampton,

Table 1. Best-fit parameters of the kinetic scheme for Kv4 channel complexes

	Kv4.2 (s^{-1})	+ DPPX (s^{-1})	+ KChIP1 (s^{-1})	Ternary (s^{-1})	z (e_0)
α	1589	3282	1443	2577	0.64
β	18.4	10	1.9	2.8	−1.31
γ	6668	7220	5556	4318	0.15
δ	2381	588	155	380	−1.21
ε	503	1101	559	466	0.07
ϕ	174	673	621	277	−0.25
k_{ci}	47	72	29	54	0
k_{ic}	0.03	0.46	0.14	0.44	0
κ_1	229	108	—	—	0
λ_1	151	34	—	—	0
κ_2	48.7	20.6	—	—	0
l_2	6.5	8.6	—	—	0

The kinetic scheme is depicted in Fig. 6*A*. The rate constants that control the voltage-dependent transitions (α, β, γ, δ, ε, ϕ) are assumed to depend exponentially on membrane potential according to the relationships $x(V) = x_0 \exp(z_X eV/kT)$, where e is the electronic charge, V is the membrane potential, k is the Boltzmann constant and T is the absolute temperature. The apparent charges (z) associated with the specific transitions were estimated from the best-fit of the ternary complex, and kept fixed in all other conditions. The allosteric factors f and g are 0.045 and 1.03, respectively, and were kept fixed.

MA, USA) software. Recordings in tsA-201 cells were most stable in the intracellular solution indicated above. To confirm that the voltage-dependent behaviour observed under these conditions was independent of the intracellular solution used, we obtained recordings from CHO cells coexpressing Kv4.2 and KChIP1 with and without DPPX-S with the same intracellular pipette solution as that used to record from cerebellar granule cells (online supplemental material, Supplementary Fig. 1). All measurements were taken at room temperature (22–24°C) and results are expressed as means ± S.E.M.

Slice preparation

All experiments were carried out in accordance with the NIH *Guide for the Care and Use of Laboratory Animals* and were approved by the New York University School of Medicine Animal Care and Use Committee.

Acute brain slices were prepared using standard techniques (Stuart *et al.* 1993). Mice (10–30 days old) were deeply anaesthetized via intraperitoneal injection of pentobarbital (100 mg (kg body weight)$^{-1}$) and decapitated. The brain was rapidly removed to oxygenated, ice-cold artificial cerebrospinal fluid (ACSF) that contained (mM): 125 NaCl, 2.5 KCl, 1.25 NaH_2PO_4, 26 $NaHCO_3$, 10 glucose, 2 $CaCl_2$ and 1 $MgSO_4$. Cutting solution was continuously bubbled with 95% O_2 and 5% CO_2 to maintain a pH of approximately 7.40. Slices (350 μm thick) were cut on a Vibratome 3000 Plus (Vibratome, St Louis, MO, USA) and incubated in a holding chamber at 32–35°C for approximately 30 min followed by continued incubation at room temperature prior to electrophysiological recording, at which point slices were transferred to a submersion-type recording chamber attached to the microscope stage and perfused with ACSF.

Patch-clamp recordings from cerebellar granule cells

Whole-cell voltage clamp recordings were performed from cerebellar granule cells using the whole-cell configuration of the patch-clamp technique (Hamill *et al.* 1981). Cells were visualized using a 40×, 0.8 NA water-immersion objective (Olympus) on an Olympus BX-50 upright microscope equipped with IR-DIC optics (Stuart *et al.* 1993). Patch electrodes (3–6 MΩ) were fashioned from borosilicate glass using an horizontal puller (Model P-97, Sutter Instrument Co., Novato, CA, USA) and filled with a solution containing (mM): 130 CH_3KO_3S (potassium methanesulphonate), 10 NaCl, 10 Hepes, 10 phosphocreatine (Tris), 2 Mg-ATP, 0.4 Na-GTP, 0.4 EGTA, 2 $MgCl_2$ and 0.16 $CaCl_2$, pH adjusted to 7.40 with KOH, and the osmolarity adjusted to 290 mosmol l^{-1} with sucrose. Membrane potentials were corrected for a 10 mV junction potential. Currents were recorded using an Axopatch 200B amplifier (Axon Instruments), lowpass filtered at 5 kHz, digitized at 16-bit resolution (Digidata 1322A; Axon Instruments) and sampled at 20 kHz. Cells with a series resistance (R_s) larger than 20 MΩ upon break-in were rejected. R_s was compensated to the extent possible (typically, 50–85% correction) and data obtained from a given cell were rejected if R_s changed by $> 20\%$ during the course of the experiment. pCLAMP 9 software (Axon Instuments) was used for data acquisition, and analysis was performed using the Clampfit module of pCLAMP.

Immunohistochemistry

For localization of Kv4.2 and Kv4.3 protein in the cerebellar cortex, mice were anaesthetized with an intraperitoneal injection of pentobarbital and transcardially perfused with 0.9% saline containing heparin (1 U ml^{-1}), followed by 30–50 ml of 0.1 M sodium phosphate buffer (NaPB; pH 7.4) containing 4% paraformaldehyde. Brains were dissected out and postfixed in the same fixative solution for 1 h at room temperature and then placed in a 30% sucrose solution at 4°C for 24 h. Frozen sagittal sections through the cerebellum, 40 μm thick, were cut on a sliding microtome and collected in phosphate-buffered saline (PBS). Sections were washed

in PBS and then incubated in a blocking solution (10% normal goat serum, 1% BSA, 0.2% cold fish gelatin, and 0.2% Triton X-100 in PBS) for 1 h at room temperature to minimize non-specific binding. Sections were then incubated with antibodies directed against Kv4.2 (10 μg ml^{-1}; mouse monoclonal anti-Kv4.2; K57/1; Neuromab; www.neuromab.org; or rabbit polyclonal directed against Kv4.2; Nadal *et al.* 2003; at 1 : 1000), or Kv4.3 (1 μg ml^{-1}; mouse monoclonal anti-Kv4.3; K75/41; Neuromab) in diluted (1 : 10) blocking solution overnight at 4°C. Following incubation with primary antibodies, sections were washed with PBS and incubated for 1 h in fluorescent Cy3-conjugated secondary antibody (goat anti-mouse or goat anti-rabbit, Jackson Immuno-Research Laboratories, Inc., West Grove, PA, USA) at room temperature. Sections were then rinsed and finally mounted using Vectashield (Vector Laboratories, Inc., Burlingame, CA, USA). Immunofluorescence images were acquired with an Olympus MVX10 microscope equipped with a Leica DFC-340FX digital camera and Leica Firecam 3.0 software. Images were transferred to a graphics program (Adobe Photoshop CS2), in which brightness and contrast were adjusted. The monoclonal and polyconal antibodies for Kv4.2 both produced the same pattern of staining in the cerebellum. Figure 2 depicts staining with the monoclonal antibody against Kv4.2.

Quantitative global kinetic modelling

Previously, we applied global kinetic modelling and a model discrimination method to explain gating of Kv4 channels quantitatively (Kaulin *et al.* 2008). Using a Chi-squared minimization function, appropriately weighted macroscopic measurements (activation, inactivation and deactivation) were evaluated simultaneously to constrain the analysis and estimate the best global-fit parameters for specific kinetic models. Here, we implemented this strategy in the new program IChMASCOT (Ion-Channel-Markov-Scheme-Optimizer; www.ichmascot.org) and assumed the kinetic scheme shown in Fig. 6*A*. This scheme is similar to those models that successfully described Kv4 gating in the study of Kaulin *et al.* (2008). In particular, these models explained the slowing of inactivation with progressive depolarization. For the sake of simplification, however, we did not include an unstable closed state connected to the open state, which reduces the open probability. Also, the scope of the kinetic analysis was limited to explain the voltage dependence of the rate of inactivation semiquantitatively. For all subunit combinations, we evaluated the following measurements simultaneously to constrain global kinetic modelling: (1) complete families of currents evoked by step depolarizations (Fig. 1); (2) the steady-state inactivation curve (not shown); and (3) the recovery from inactivation (Fig. 1*F*). For display, model simulations were performed in the program IChSimlab (www.ichmascot.org).

Results

Voltage dependence of inactivation of Kv4.2 channels in heterologous expression systems

Previous studies of the influence of KChIP and DPPL proteins on the properties of Kv4 channels have primarily used two-microelectrode voltage-clamp in the *Xenopus* oocyte expression system (Nadal *et al.* 2003, 2006; Jerng *et al.* 2005). To minimize the variability that methodological differences may introduce and facilitate comparison with the properties of native neuronal channels, we chose to express the Kv4 channel complexes in a mammalian heterologous expression system and obtain the currents with the same recording method (whole-cell patch-clamp).

The currents produced by expression of Kv4.2 proteins alone, were compared to those resulting from coexpression of Kv4.2 with the accessory subunits KChIP1 and DPPX-S (Fig. 1). Records of the currents recorded during step depolarizations from tsA-201 cells transfected with Kv4.2 alone, Kv4.2 plus KChIP1, Kv4.2 plus DPPX-S and Kv4.2 with both KChIP1 and DPPX-S are shown in Fig. 1*A–D*. As previously reported, KChIP1 slows down current inactivation and induces more complete inactivation by the end of the voltage pulse, and DPPX accelerates the overall channel kinetics (An *et al.* 2000; Beck *et al.* 2002; Nadal *et al.* 2003; reviewed in Jerng *et al.* 2004*a*). In Fig. 1*E* we compare the rate of inactivation as a function of voltage for the four conditions from a number of cells. As reported before, the currents mediated by Kv4 channels decay with a complex multiexponential time course (Jerng & Covarrubias, 1997; Bahring *et al.* 2001; Jerng *et al.* 2004*b*). Since the number of exponentials that may describe the decay varies depending on subunit composition, we used the time at which half of the peak current is inactivated (half-inactivation time or $t_{1/2}$) to compare inactivation kinetics under different conditions. This model-independent strategy has been previously used by us and others to compare the inactivation kinetics of Kv4 currents (Nadal *et al.* 2001, 2003; Jerng *et al.* 2007).

In cells transfected with Kv4.2 alone, the rate of inactivation does not slow down during large depolarizations (Fig. 1*E*). In sharp contrast, the voltage dependence of the rate of inactivation of Kv4.2 channels cotransfected with KChIP1 exhibits a transition from an accelerating rate of inactivation at negative voltages to a decelerating rate at positive membrane potentials (Fig. 1*E*). In the presence of KChIP1, the $t_{1/2}$ reaches a minimum between −40 and −10 mV; then, it increases with a slope of approximately 2.3 ms/10 mV (0 to +60 mV; Fig. 1*E*). As previously reported, DPPX-S alone speeds

up the inactivation rate significantly. The differences between the $t_{1/2}$ of Kv4.2 currents in cells coexpressing DPPX and cells expressing Kv4.2 channels alone are most prominent at membrane potentials more negative than ~0 mV (Fig. 1*E*). Furthermore, the $t_{1/2}$ of the currents in the presence of DPPX (without KChIP) does not increase with large depolarizations. However, inactivation slows down with increasing depolarization in cells transfected with both KChIP1 and DPPX-S with a slope of 2.9 ms/10 mV (measured between 0 and +60 mV). This slope is slightly steeper than that observed in cells cotransfected with KChIP1 only, but the main difference between the two conditions is in the rate of inactivation in the most negative voltage range. In cells expressing both auxiliary subunits, DPPX-S clearly accelerates the rate of inactivation between −60 and −10 mV, and thereby significantly broadens the voltage range over which the rate of inactivation decreases with increasing depolarization. Similar voltage dependence profiles were obtained in transfected CHO cells (Supplementary Fig. 1). The curves in Fig. 1*E* demonstrate that the relation between inactivation rate and membrane potential is distinct for the four conditions tested in these experiments. Therefore, subunit composition dictates Kv4 channel inactivation kinetics. The specific contributions of DPPX-S to Kv4.2 gating are also apparent when comparing the recoveries from inactivation (Fig. 1*F*). The ternary complex exhibits fast recovery from inactivation ($\tau = 45$ ms) that is already set by the interaction between Kv4.2 and DPPX-S in the binary complex ($\tau = 40$ ms).

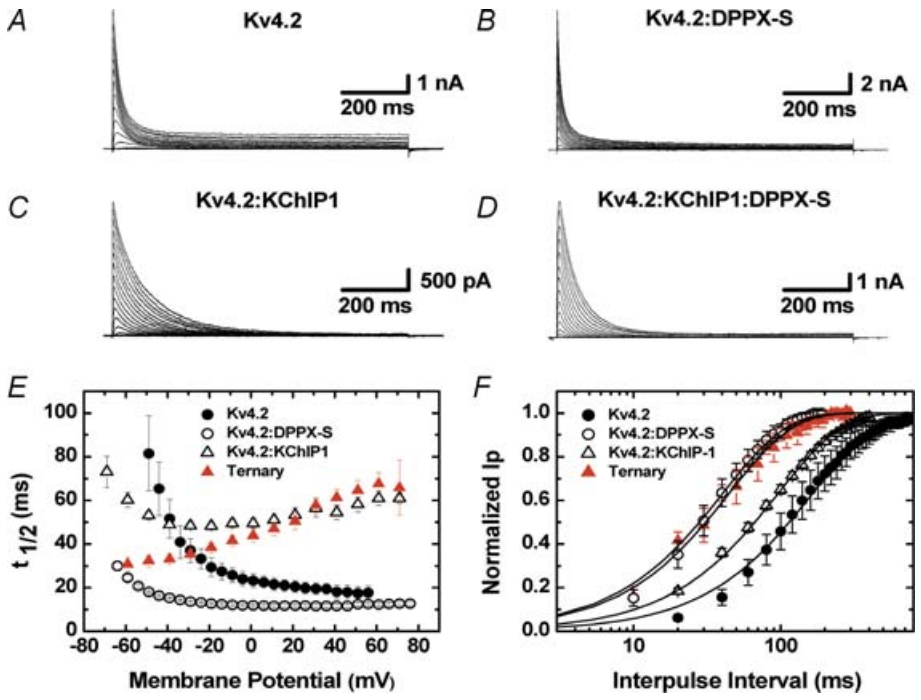

Figure 1. Modulation of the inactivation kinetics of Kv4.2 channels by associated proteins KChIP1 and DPPX-S

A–D, whole-cell K^+ currents from tsA-201 cells transfected with Kv4.2 (*A*), Kv4.2 and DPPX-S (*B*), Kv4.2 and KChIP1 (*C*) or Kv4.2 + KChIP1 and DPPX-S (*D*), evoked by step depolarizations from −109 to +61 mV in 10 mV increments from a holding potential of −149 mV. Note that DPPX accelerates and KChIP1 slows down inactivation kinetics. *E*, voltage dependence of the rate of inactivation of Kv4.2 channels. Plots of the half-inactivation time ($t_{1/2}$) against membrane potential from the currents recorded in tsA-201 cells expressing Kv4.2 alone (●), Kv4.2 and DPPX-S (○), Kv4.2 and KChIP1 (△) and Kv4.2 plus KChIP1 and DPPX-S (grey triangles). Shown are means S.E.M. ($n = 4$, 4, 10 and 10, respectively). Note that, for currents recorded in the presence of KChIP1 and KChIP1 plus DPPX-S, the rate of inactivation increases with strong depolarizations. However, DPPX accelerates the rate of inactivation between −60 and −10 mV, increasing the voltage range over which the $t_{1/2}$ increases with progressive depolarization. *F*, recoveries from inactivation of Kv4.2 alone (●), Kv4.2 and DPPX-S (○), Kv4.2 and KChIP1 (△) and Kv4.2 plus KChIP1 and DPPX-S (grey triangles); the recovery voltages were −115, −128, −140 and −140 mV, respectively. These voltages were adjusted to account for shifts in the voltage dependence of steady-state inactivation (not shown), and therefore are 40 mV more negative than the midpoint voltage of the corresponding steady-state inactivation curve. The curves shown are means S.E.M. ($n = 3$, 3, 8 and 9, respectively) and the lines are best-fit single exponentials with the following time constants: 165, 40, 96 and 45 ms, for Kv4.2, Kv4.2:DPPX-S, Kv4.2:KChIP-1 and Kv4.2:KChIP-1:DPPX-S, respectively.

Kv4.2 and Kv4.3 proteins in mouse cerebellar granule cells

Cerebellar granule neurons have a large I_{SA}, consistent with prominent expression of Kv4.2 and Kv4.3 mRNAs and proteins (Serodio & Rudy, 1998; Rhodes *et al.* 2004; Strassle *et al.* 2005). They are also among the few neuronal populations where the patterns of expression of the various molecular components of Kv4 channels have been analysed with good cellular resolution (Nadal *et al.* 2003; Rhodes *et al.* 2004; Strassle *et al.* 2005; Zagha *et al.* 2005; Jerng *et al.* 2007). Moreover, compared to other neurons, cerebellar granule cells are elecrotonically compact due to the small size of these cells (~5 μm) and the short length of dendritic processes, allowing good voltage control for whole cell recording (Cull-Candy *et al.* 1989). We therefore selected these neurons to investigate the properties of native neuronal I_{SA} for comparison with the currents heterologously expressed in mammalian cells.

In situ hybridization and immunohistochemical studies in rat brain showed reciprocal gradients of expression of Kv4 mRNA transcripts and protein products, with Kv4.2 being expressed most prominently in anterior cerebellar lobules and Kv4.3 in posterior lobules and the flocculonodular lobe (Serodio & Rudy, 1998; Hsu *et al.* 2003; Strassle *et al.* 2005). We used immunohistochemistry with Kv4.2- and Kv4.3-specific antibodies to explore whether this is also the case in mouse cerebellar cortex. Immunohistochemical analysis of Kv4.2 and Kv4.3 protein expression shows a similar pattern of expression for the channel proteins in the mouse cerebellar cortex (Fig. 2). Since there are small but consistent differences in the properties of Kv4.2 and Kv4.3 channels in heterologous expression systems (Serodio *et al.* 1996), we targeted for electrophysiological recording and analysed separately the currents in cerebellar granule cells from anterior and posterior lobules to characterize either Kv4.2- or Kv4.3-dominated native currents, respectively.

Isolation and characterization of the I_{SA} in cerebellar granule cells

Classical strategies for the isolation of native A-type currents from neurons have used prepulse protocols to inactivate the A-type K^+ current, which is then obtained by subtraction of the current remaining after the prepulse from the total current (e.g. Connor & Stevens, 1971; Rudy *et al.* 1988; Cull-Candy *et al.* 1989). The outward current in granule cells includes a slowly inactivating component, which increased in amplitude with age and can be large relative to the transient component, particularly in anterior lobules (Fig. 3). We found that in slices from mice older than P12, the classical protocol was not useful to isolate the I_{SA} from cerebellar granule cells, except during relatively small depolarizations, because the prepulse also inactivated a significant amount of the slowly inactivating components of the total outward current. Contamination of the I_{SA} with slowly inactivating components suppressed by the prepulse was particularly large (but not exclusive) for cells in anterior lobules. Similar difficulties were found in previous attempts at isolating the I_{SA} from cerebellar granule cells in rat, and past studies have often focused on characterizing the current during small depolarizations (Cull-Candy *et al.* 1989).

Cerebellar granule cells prominently express the Kv3 subunit Kv3.1 (Perney *et al.* 1992; Weiser *et al.* 1994; Weiser *et al.* 1995; Sekirnjak *et al.* 1997). Kv3 channels activate in a voltage range positively shifted compared to Kv4 channels, as is the case with the slowly inactivating component

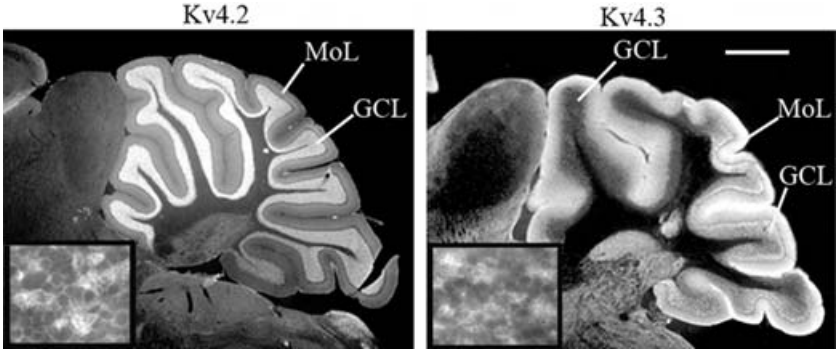

Figure 2. Immunolocalization of Kv4.2 and Kv4.3 proteins in the mouse cerebellar cortex
Immunostaining of sagittal sections of the mouse cerebellum with antibodies to Kv4.2 and Kv4.3. The figure shows the Cy3 fluorescence signal. Kv4.2 is expressed predominantly in the granule cell layer (GCL); with prominent staining in anterior, but weak staining in posterior lobules. Kv4.3 is strongly expressed in the molecular layer (MoL), where the dendrites of Purkinje cells are brightly stained. In the granule cell layer (GCL) Kv4.3 immunostaining is prominent in posterior lobules and extremely weak in anterior lobules. Insets show higher magnification images of the GCL illustrating Kv4.2 and Kv4.3 labelling in the periphery of granule cell somata and in the glomeruli containing the dendritic processes of the granule cells. Scale bar: 800 μm; insets: 30 μm.

in cerebellar granule cells. It is likely that much of this component of the outward current in these neurons is mediated by Kv3 channels. We therefore utilized relatively low concentrations of TEA (5 mM), a drug that does not block Kv4 channels but completely blocks Kv3 channels (Coetzee *et al.* 1999), to block the slow inactivating component of the current in cerebellar granule cells and facilitate the isolation of the I_{SA}. This concentration of TEA blocked a major portion of the total outward current in cerebellar granule cells, leaving a highly enriched I_{SA} (Fig. 3*C* and *D*). A higher concentration of TEA (20 mM) gave identical results. Since TEA was used for many of the recordings in heterologous cells in order to block a current intrinsic to the tsA-201 cells, recording in the presence of TEA in cerebellar granule cells also allowed a better comparison of the native and the reconstituted currents.

Voltage dependence of the rate of inactivation in cerebellar granule cells

In the presence of TEA a prepulse protocol could be applied to isolate the I_{SA} (Fig. 4). A 1–5 s prepulse to −40 mV inactivated the entire transient component. The remaining current may represent the 'standing outward current', a current mediated by two pore K^+ channels (K2P), and/or could be mediated by TEA-insensitive non-inactivating Kv1 channels (Millar *et al.* 2000; Mathie *et al.* 2003). The current suppressed by the prepulse, obtained by subtraction, inactivated nearly completely (Fig. 4*A* and *B*, lower traces), and was used to characterize the properties of the I_{SA} in cerebellar granule cells. This I_{SA} was nearly eliminated by 10 mM 4-AP (Supplementary Fig. 2), a characteristic inhibitor of Kv4-mediated A-type currents at millimolar concentrations (Coetzee *et al.* 1999). Figure 4*E* compares the conductance–voltage relation and the voltage dependence of inactivation for the currents recorded in anterior *versus* posterior lobules, and Fig. 4*F*, the recovery from inactivation at −120 mV for the two cell types. The properties of the currents in the two cell types are very similar, but showed minor differences, consistent with the differences reported between Kv4.2 and Kv4.3 currents in heterologous cells (Serodio *et al.* 1996).

We measured the inactivation $t_{1/2}$ against voltage from a number of neurons in anterior and posterior cerebellar lobules and the results are plotted in Fig. 4*C* and *D*. The plots show that the rate of inactivation of the I_{SA} isolated through these procedures has voltage dependence similar to that seen in heterologously expressed Kv4 channels in the presence of KChIP-1 and DPPX-S. This is observed for the currents in both Kv4.2- and Kv4.3-containing granule neurons. The slope of the $t_{1/2}$–voltage relation (2.6 ms/10 mV and 2.5 ms/10 mV for anterior and posterior lobules, respectively) and the overall profile of the voltage dependence of the inactivation rates are remarkably similar to those observed for the currents expressed by the ternary Kv4 channel containing Kv4.2, KChIP-1 and DPPX-S in heterologous cells.

To confirm that the observed behaviour is not the result of isolating a current containing two or more components with different voltage dependencies inactivating at different rates, we took advantage of the fast rate of recovery of Kv4-mediated transient currents compared to other fast inactivating K^+ channels. If the values of the time constants of inactivation as a function of voltage are a feature of a single population of independent channels that recover rapidly from inactivation, we would expect their values to be the same for a partially or a fully recovered set of channels. We applied depolarizing pulses to different membrane potentials (test pulses) following a prepulse to +10 mV applied at different times before the test pulse. Between the two pulses the membrane was held at -110 mV. The $t_{1/2}$–voltage relations of the currents obtained during the test pulses following different recovery times are shown in Fig. 5*C* and *D*, along with those of the currents elicited by the same depolarizations in the absence of a prepulse. The $t_{1/2}$–voltage relations of fully or partially recovered currents overlap at all membrane potentials and recovery periods, indicating that they reflect a homogeneous population of channels with identical recovery time course.

Kinetic modelling of the voltage dependence of inactivation kinetics in Kv4.2 channels

The unusual voltage dependence of inactivation described here can be explained by assuming preferential closed-state inactivation (Klemic *et al.* 1998; Kaulin *et al.* 2008) and

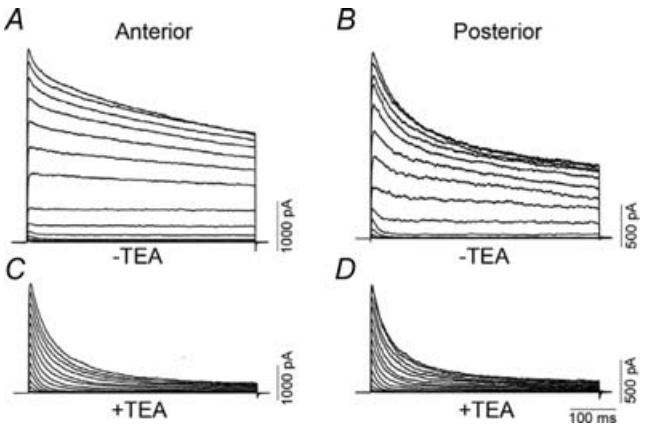

Figure 3. K^+ currents in cerebellar granule cells
Whole-cell ionic currents recorded in a representative cerebellar granule cell from an anterior (*A* and *C*) or a posterior (*B* and *D*) lobule, before (*A* and *B*) or after (*C* and *D*) the application of 5 mM TEA. Currents were recorded in the presence of 500 nM TTX and were elicited by step depolarizations from −90 to +60 mV in 10 mV increments from a holding potential of −130 mV.

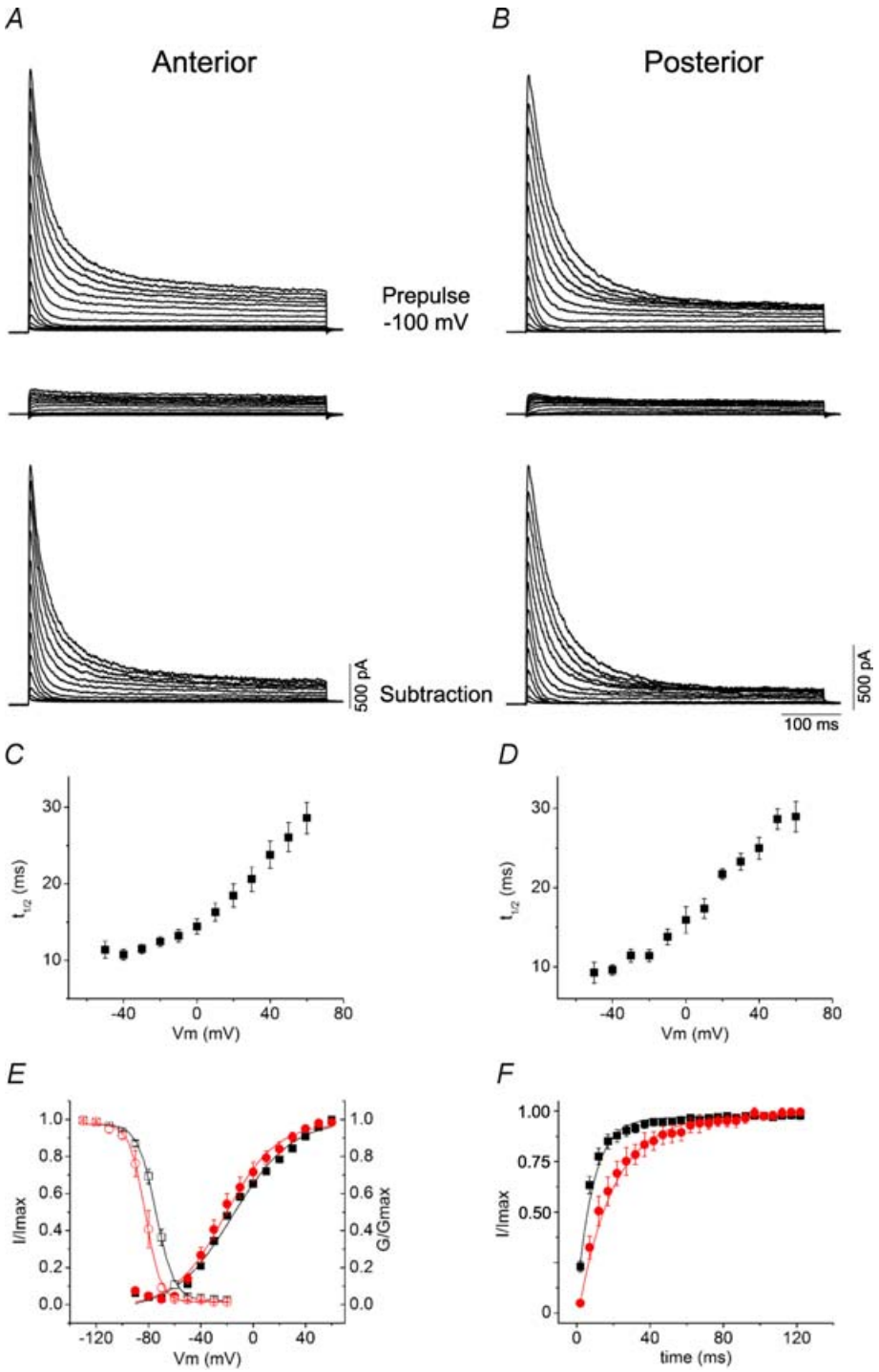

Figure 4. Inactivation kinetics of I_{SA} in cerebellar granule cells
A and *B*, whole-cell K^+ currents recorded in a representative cerebellar granule cell from an anterior (*A*) or a posterior (*B*) lobule recorded in the presence of 5 mM TEA. Shown are the currents elicited by step depolarizations from −90 to +60 mV in 10 mV increments, preceded by a prepulse to −100 mV from a holding potential of −130 mV (upper traces) or a prepulse to −40 mV (middle traces). The lower traces show the transient currents (I_{SA}) obtained by subtracting the currents recorded during depolarizing steps preceded by a prepulse to −40 mV from the currents obtained during depolarizing steps preceded by a prepulse to −100 mV. *C* and *D*, half-inactivation time ($t_{1/2}$) as a function of membrane potential of the I_{SA} obtained in cerebellar granule cells from anterior (*C*) and posterior (*D*) lobules. Shown are means S.E.M. ($n = 17$ for anterior and $n = 6$ for posterior lobules). *E*, normalized peak conductance–voltage relations (G/G_{max}) and steady-state inactivation curves (I/I_{max}) for granule cells recorded in anterior (squares) and posterior (circles) cerebellar lobules. Peak conductance (G) was calculated as

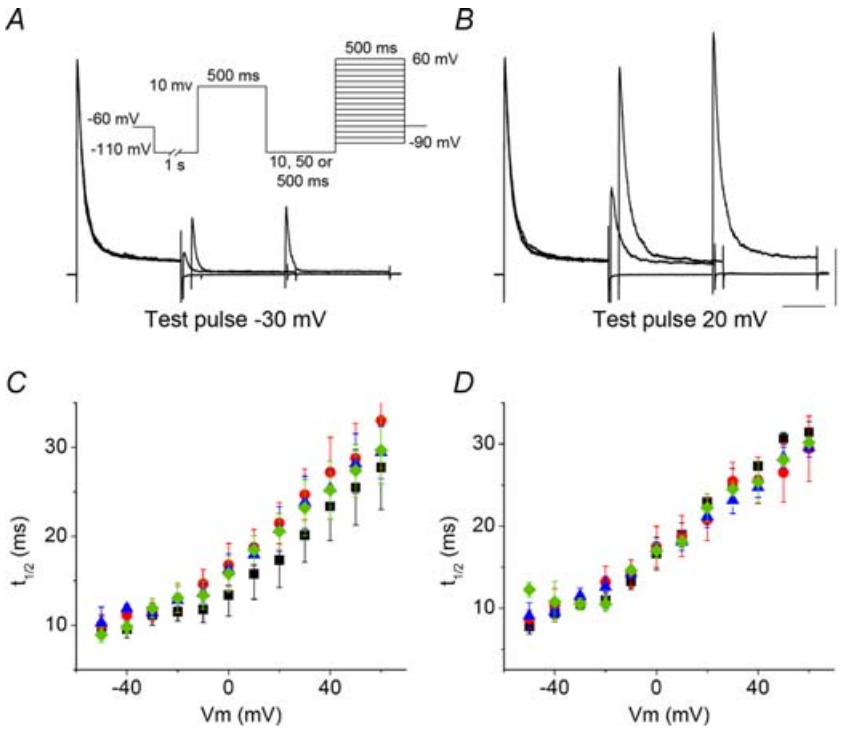

Figure 5. The voltage dependence of the rate of inactivation of the I_{SA} in cerebellar granule cells is a property of a homogeneous population of channels
A and *B*, representative records of the currents used to determine inactivation rates. Shown are the currents recorded during a test pulse to −30 mV (*A*) or +20 mV (*B*) preceded by a prepulse to +10 mV applied 10, 50 or 500 ms before the test pulse. Between the prepulse and the test pulse the cell was held at −110 mV. *C* and *D*, half-inactivation time ($t_{1/2}$) as a function of membrane potential of the I_{SA} obtained in cerebellar granule cells from anterior (*C*) and posterior (*D*) lobules during test pulses to the indicated voltages after a 10 ms (diamonds), 50 ms (triangles), or 500 ms (circles) recovery period at −110 mV from the inactivation produced by a prepulse to +10 mV. Black squares are the $t_{1/2}$ for the currents recorded during identical test pulses in the absence of a prepulse. Shown are means S.E.M. ($n = 4$ for anterior and $n = 3$ for posterior lobules).

a weakly voltage-dependent opening step, a feature proposed for several types of voltage-gated K^+ channels (Zagotta *et al.* 1994; Klemic *et al.* 1998; Schoppa & Sigworth, 1998; Smith-Maxwell *et al.* 1998). Thus, if inactivation takes place preferentially from the preopen closed but activated state, further membrane depolarization acting on a weakly voltage-dependent opening step would gradually increase the open probability and hence decrease the probability of residing in the inactivation-permissive preopen closed state. Consequently, the observed rate of macroscopic inactivation decreases at strongly depolarized membrane potentials.

To test these ideas, we applied the Kv4 kinetic model proposed by Kaulin *et al.* (2008), and assumed that Kv4.2 and Kv4.2:DPPX-S channels undergo open-state inactivation, whereas the presence of KChIP-1 precludes open-state inactivation in Kv4.2:KChIP-1 and ternary Kv4.2 channels (Methods; Fig. 6*A*). Thus, Kv4.2 channel complexes that include KChIP-1 undergo preferential closed-state inactivation. Under these conditions, the kinetic model accounted for the observations from all subunit combinations closely (Fig. 6*B* and *C*). In particular, this model produced excellent descriptions of the $t_{1/2}$–voltage relations (derived from the best-fit currents; Fig. 7*A*). As expected, the rate of inactivation increases with depolarization and levels off when there is open-state inactivation strictly coupled to activation; and conversely, the rate of inactivation decreases with depolarization when channels undergo preferential closed-state inactivation. In the latter case, the weakly voltage-dependent opening equilibrium is critical because otherwise the inactivation rate exhibits little or no voltage dependence (Fig. 7*B*). The theoretical $t_{1/2}$–voltage relation of the ternary Kv4.2 complex with a slope of 2.9 ms/10 mV recapitulates the behaviour of native I_{SA} in cerebellar granule neurons (2.6 ms/10 mV). Moreover, the model produced an excellent description of the recoveries from inactivation for all subunit combinations (Fig. 7*C*).

Discussion

Here, we showed that the rate of inactivation of the I_{SA} in mouse cerebellar granule neurons has unusual voltage

$G = I_p/(V_m - V_{eq})$, where I_p, V_m and V_{eq} are the peak current, the test potential and the K^+ equilibrium potential, respectively. Shown are means S.E.M. ($n = 21$ for anterior and $n = 6$ for posterior lobules). The continuous lines across the data points are the best-fits to Boltzmann functions with a $V_{1/2} = -74$ and −82 mV a slope factor $k = 6.9$ and 5.9 mV for the inactivation curves in anterior and posterior lobules, respectively; and a $V_{1/2} = -15$ and −21 mV a slope factor $k = 22$ and 19 mV for the conductance–voltage curves in anterior and posterior lobules, respectively. *F*, recovery from inactivation of I_{SA} at −130 mV in cells recorded from anterior (squares) and posterior (circles) lobules. Shown are means S.E.M. ($n = 11$ for anterior and $n = 6$ for posterior lobules). The traces are single exponential fits through the data.

dependence that appears to be a property of a homogeneous population of channels and resembles the voltage dependence of the rate of inactivation of Kv4.2 channels expressed in heterologous mammalian cells containing the accessory subunits KChIP-1 and DPPX-S.

I_{SA} channels in mouse cerebellar granule cells are likely ternary complexes containing accessory subunits KChIP and DPPX

Using biochemical methods, KChIPs and DPPLs were initially discovered as proteins that associate with Kv4 proteins, the pore-forming subunits mediating most of the somatodendritic I_{SA} in neurons. KChIPs were isolated in a yeast two-hybrid screen that used the amino terminus of Kv4.2 as bait (An *et al.* 2000). Association of KChIPs with native Kv4 channel complexes in brain was subsequently demonstrated by co-immunoprecipitation. Association of DPPX with Kv4 channels in brain tissue was discovered by immunopurification of Kv4 channel complexes from rat cerebellar membranes using Kv4.2 antibodies (Nadal *et al.* 2003). These channel complexes were also shown to contain KChIP proteins (Nadal *et al.* 2003).

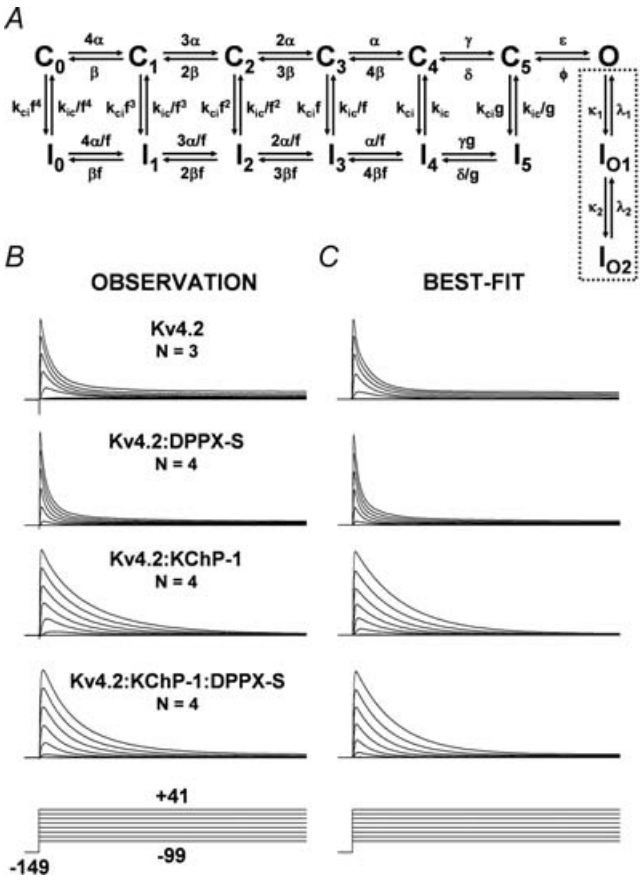

Figure 6. Kinetic modelling of Kv4.2 currents
A, kinetic scheme for Kv4.2 channel gating based on the models proposed by Kaulin *et al.* (2008). To obtain the model's best-fit for each condition, the analysis was constrained simultaneously by all traces in the average family of currents, the average steady-state inactivation curve (not shown) and the average recovery from inactivation (Fig. 1*F* and Methods). The open-state inactivation pathway is enclosed in a box (dashed lines). *B* and *C*, families of observed (*B*) and best-fit (*C*) currents elicited by step depolarizations from −99 to +41 mV in 20 mV increments from a holding potential of −149 mV. The number of averaged families of observed currents is indicated in the plots. The best-fit parameters are shown in Table 1.

KChIPs and DPPX (or its homologue DPP10) have powerful effects on the expression and biophysical properties of Kv4 channels expressed in heterologous cells (An *et al.* 2000; Nadal *et al.* 2003, 2006; Jerng *et al.* 2005; Ren *et al.* 2005; Zagha *et al.* 2005; Dougherty & Covarrubias, 2006; Jerng *et al.* 2007). KChIPs and DPPLs facilitate the transport of Kv4 channels to the plasma membrane, which are otherwise retained in intracellular compartments. These proteins also have major effects on the biophysical properties of the channels. KChIPs slow down and DPPLs accelerate the rate of inactivation, while both accessory subunits speed up recovery from inactivation. In addition, DPPLs produce large shifts in the voltage dependence of activation and inactivation. The currents recorded in heterologous cells expressing the ternary complex containing Kv4 pore forming subunits as well as KChIPs and DPPLs more closely resemble several properties of the I_{SA} in various neuronal populations (Nadal *et al.* 2003; Jerng *et al.* 2005, 2007; Zagha *et al.* 2005), supporting the notion that the native channels mediating the somatically recorded I_{SA} contain these accessory proteins. In addition, KChIPs and DPPX are expressed prominently in neuronal brain populations that also express significant levels of Kv4.2 or Kv4.3 proteins, and with similar subcellular distributions (Nadal *et al.* 2003; Rhodes *et al.* 2004; Strassle *et al.* 2005; Zagha *et al.* 2005) (B. Clark, E. Kwon & B. Rudy, unpublished observations). Furthermore, in Kv4.2 knock-out mouse there is a region- and cell-specific down-regulation of individual KChIP auxiliary subunits (Menegola & Trimmer, 2006) and DPPX in brain (J. Trimmer, personal communication).

Here, we show that the voltage dependence of the rate of inactivation in cerebellar granule neurons closely matches the voltage dependence of the inactivation rate of the currents observed in heterologous mammalian cells expressing the ternary complex containing Kv4.2, KChIP-1 and DPPX-S. KChIP-1 is largely responsible for the large decrease in the rate of inactivation during large depolarizations. However, the studies in heterologous cells demonstrate that the voltage dependence of the inactivation rate is different in Kv4.2-KChIP channels in the presence or absence of DPPX-S (Fig. 1). The $t_{1/2}$–voltage relation for the I_{SA} in cerebellar granule neurons is very similar to that obtained in heterologous cells expressing both accessory proteins (compare Figs 4 and 5 with Fig. 1). The reconstitution of this complex and unique behaviour (among A-type K^+ currents) by

the ternary complex containing Kv4, DPPX and KChIP proteins provides additional strong evidence in favour of somatically recorded I_{SA} being mediated by Kv4 channels that contain both types of accessory proteins.

I_{SA} channels in mouse cerebellar granule neurons inactivate preferentially from closed states

The mechanisms of inactivation of Kv4-mediated I_{SA} channels remain poorly understood and seem to be mechanistically different from those in other inactivating voltage-gated K^+ channels (Jerng *et al.* 2004*a*). Previous studies have proposed closed-state inactivation as a significant pathway of inactivation in Kv4 channels (Jerng *et al.* 1999; Bahring *et al.* 2001; Beck & Covarrubias, 2001; Beck *et al.* 2002; Shahidullah & Covarrubias, 2003; Kaulin *et al.* 2007). Although Kv4 channels expressed without KChIPs exhibit a fast open-state N-type-like mechanism of inactivation (Gebauer *et al.* 2004), KChIPs preclude this mechanism because they sequester the N-terminal inactivation gate (Beck *et al.* 2002; Pioletti *et al.* 2006; Wang *et al.* 2007). It is therefore believed that Kv4 channel complexes that include KChIPs inactivate preferentially from closed states (Callsen *et al.* 2005; Kaulin *et al.* 2008). However, the importance of this pathway in Kv4 channels has remained controversial (Patel & Campbell, 2005; S. Wang *et al.* 2005).

The voltage dependence of the inactivation rate described here is predicted by kinetic models of closed-state inactivation (Klemic *et al.* 1998, 2001; Kaulin *et al.* 2007). The rate of inactivation decreases with depolarization once voltage-dependent activation is complete because further depolarization promotes the weakly voltage-dependent opening step, which decreases the probability of channels residing in the inactivation-permissive preopen closed state. A weakly voltage-dependent opening step is therefore critical in this mechanism. The observation that the inactivation rates of the I_{SA} in cerebellar granule neurons decrease with depolarization at positive membrane potentials further supports the view that native Kv4 channels also inactivate preferentially from closed-states.

Closed-state inactivation in Kv4 channels is probably the mechanism that regulates the availability of the channels at subthreshold membrane potentials, and is optimally fast in this range of membrane potentials.

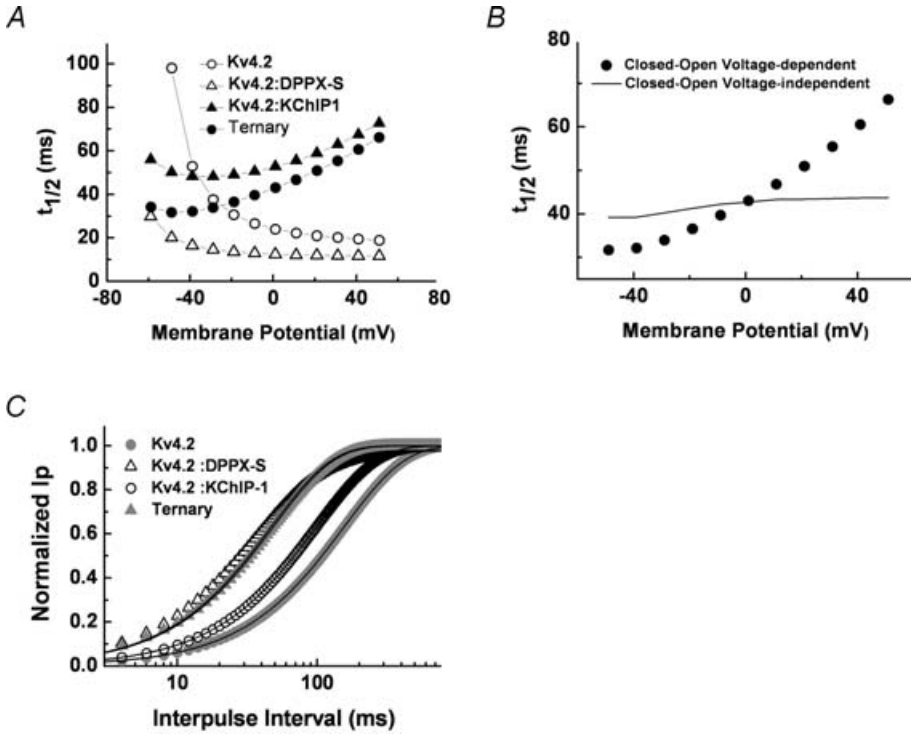

Figure 7. Kinetic modelling of Kv4.2 inactivation
A, plots of half-inactivation time against voltage ($t_{1/2}$–voltage relation) for simulated currents mediated by Kv4.2 channels with different subunit compositions. The $t_{1/2}$ was obtained from the best-fit currents shown in Fig. 6*C*. *B*, effect of voltage dependence of the opening equilibrium on the $t_{1/2}$–voltage relation. In one case (●), the rate constants ε and ϕ are voltage-dependent (Fig. 6*A*; Table 1), and in the other (continuous line), these rate constants are assumed to be voltage-independent. All other best-fit parameters are kept as depicted in Table 1. *C*, best-fit recoveries from inactivation of Kv4.2 channels with different subunit compositions. Continuous lines are best single exponential fits with the following time constants: 156 ms (Kv4.2); 47 ms (Kv4.2:DPPX-S); 99 ms (Kv4.2:DPPX-S); and 49 ms (Ternary). These values are in excellent agreement with the experimental observations (Fig. 1 legend).

Although at typical neuronal resting membrane potentials (−60 mV) these channels are mostly inactivated at steady state, a brief conditioning hyperpolarization will recruit them because their recovery from inactivation is fast. Then, activation of Kv4 channels by a subsequent depolarization will delay firing of the action potential. The characteristically fast voltage-dependent recovery from inactivation of native Kv4 channel complexes distinguishes them from other Kv channels that inactivate primarily via classical N-type and P/C-type mechanisms. This hallmark of Kv4 channel complexes might be a direct consequence of the mechanism responsible for closed-state inactivation, which remains unknown. The slowing of inactivation with depolarization may confer another role. By inactivating more slowly at depolarized membrane potentials, Kv4 channels could have a greater impact on spike repolarization.

References

Adams JP, Anderson AE, Varga AW, Dineley KT, Cook RG, Pfaffinger PJ & Sweatt JD (2000). The A-type potassium channel Kv4.2 is a substrate for the mitogen-activated protein kinase ERK. *J Neurochem* **75**, 2277–2287.

An WF, Bowlby MR, Betty M, Cao J, Ling HP, Mendoza G, Hinson JW, Mattsson KI, Strassle BW, Trimmer JS & Rhodes KJ (2000). Modulation of A-type potassium channels by a family of calcium sensors. *Nature* **403**, 553–556.

Bahring R, Boland LM, Varghese A, Gebauer M & Pongs O (2001). Kinetic analysis of open- and closed-state inactivation transitions in human Kv4.2 A-type potassium channels. *J Physiol* **535**, 65–81.

Beck EJ, Bowlby M, An WF, Rhodes KJ & Covarrubias M (2002). Remodelling inactivation gating of Kv4 channels by KChIP1, a small-molecular-weight calcium-binding protein. *J Physiol* **538**, 691–706.

Beck EJ & Covarrubias M (2001). Kv4 channels exhibit modulation of closed-state inactivation in inside-out patches. *Biophys J* **81**, 867–883.

Callsen B, Isbrandt D, Sauter K, Hartmann LS, Pongs O & Bähring R (2005). Contribution of N- and C-terminal Kv4.2 channel domains to KChIP interaction. *J Physiol* **568**, 397–412.

Chen X, Yuan LL, Zhao C, Birnbaum SG, Frick A, Jung WE, Schwarz TL, Sweatt JD & Johnston D (2006). Deletion of Kv4.2 gene eliminates dendritic A-type K^+ current and enhances induction of long-term potentiation in hippocampal CA1 pyramidal neurons. *J Neurosci* **26**, 12143–12151.

Coetzee WA, Amarillo Y, Chiu J, Chow A, Lau D, McCormack T, Moreno H, Nadal MS, Ozaita A, Pountney D, Saganich M, Vega-Saenz de Miera E & Rudy B (1999). Molecular diversity of K^+ channels. *Ann N Y Acad Sci* **868**, 233–285.

Connor JA & Stevens CF (1971). Prediction of repetitive firing behaviour from voltage clamp data on an isolated neurone soma. *J Physiol* **213**, 31–53.

Cull-Candy SG, Marshall CG & Ogden D (1989). Voltage-activated membrane currents in rat cerebellar granule neurones. *J Physiol* **414**, 179–199.

Dougherty K & Covarrubias M (2006). A dipeptidyl aminopeptidase-like protein remodels gating charge dynamics in Kv4.2 channels. *J Gen Physiol* **128**, 745–753.

Franqueza L, Valenzuela C, Eck J, Tamkun MM, Tamargo J & Snyders DJ (1999). Functional expression of an inactivating potassium channel (Kv4.3) in a mammalian cell line. *Cardiovasc Res* **41**, 212–219.

Gebauer M, Isbrandt D, Sauter K, Callsen B, Nolting A, Pongs O & Bahring R (2004). N-type inactivation features of Kv4.2 channel gating. *Biophys J* **86**, 210–223.

Hamill OP, Marty A, Neher E, Sakmann B & Sigworth FJ (1981). Improved patch-clamp techniques for high-resolution current recording from cells and cell-free membrane patches. *Pflugers Arch* **391**, 85–100.

Hille B (2001). *Ion Channels of Excitable Membranes*, 3rd edn. Sinauer Associates, Inc., Sunderland, MA, USA.

Hoffman DA, Magee JC, Colbert CM & Johnston D (1997). K^+ channel regulation of signal propagation in dendrites of hippocampal pyramidal neurons. *Nature* **387**, 869–875.

Hsu YH, Huang HY & Tsaur ML (2003). Contrasting expression of Kv4.3, an A-type K^+ channel, in migrating Purkinje cells and other post-migratory cerebellar neurons. *Eur J Neurosci* **18**, 601–612.

Hu HJ, Carrasquillo Y, Karim F, Jung WE, Nerbonne JM, Schwarz TL & Gereau RW 4th (2006). The Kv4.2 potassium channel subunit is required for pain plasticity. *Neuron* **50**, 89–100.

Jerng HH & Covarrubias M (1997). K^+ channel inactivation mediated by the concerted action of the cytoplasmic N- and C-terminal domains. *Biophys J* **72**, 163–174.

Jerng HH, Kunjilwar K & Pfaffinger PJ (2005). Multiprotein assembly of Kv4.2, KChIP3 and DPP10 produces ternary channel complexes with ISA-like properties. *J Physiol* **568**, 767–788.

Jerng HH, Lauver AD & Pfaffinger PJ (2007). DPP10 splice variants are localized in distinct neuronal populations and act to differentially regulate the inactivation properties of Kv4-based ion channels. *Mol Cell Neurosci* **35**, 604–624.

Jerng HH, Pfaffinger PJ & Covarrubias M (2004*a*). Molecular physiology and modulation of somatodendritic A-type potassium channels. *Mol Cell Neurosci* **27**, 343–369.

Jerng HH, Qian Y & Pfaffinger PJ (2004*b*). Modulation of Kv4.2 channel expression and gating by dipeptidyl peptidase 10 (DPP10). *Biophys J* **87**, 2380–2396.

Jerng HH, Shahidullah M & Covarrubias M (1999). Inactivation gating of Kv4 potassium channels: molecular interactions involving the inner vestibule of the pore. *J Gen Physiol* **113**, 641–660.

Johnston D, Christie BR, Frick A, Gray R, Hoffman DA, Schexnayder LK, Watanabe S & Yuan LL (2003). Active dendrites, potassium channels and synaptic plasticity. *Philos Trans R Soc Lond B Biol Sci* **358**, 667–674.

Johnston D, Hoffman DA, Magee JC, Poolos NP, Watanabe S, Colbert CM & Migliore M (2000). Dendritic potassium channels in hippocampal pyramidal neurons. *J Physiol* **525**, 75–81.

Kaulin Y, De Santiago-Castillo JA, Rocha C & Covarrubias M (2008). Mechanism of the modulation of Kv4:KChIP-1 channels by elevated external K^+. *Biophys J* **94**, 1241–1251.

Kim J, Jung SC, Clemens AM, Petralia RS & Hoffman DA (2007). Regulation of dendritic excitability by activity-dependent trafficking of the A-type K^+ channel subunit Kv4.2 in hippocampal neurons. *Neuron* **54**, 933–947.

Kim J, Wei DS & Hoffman DA (2005). Kv4 potassium channel subunits control action potential repolarization and frequency-dependent broadening in rat hippocampal CA1 pyramidal neurones. *J Physiol* **569**, 41–57.

Klee R, Ficker E & Heinemann U (1995). Comparison of voltage-dependent potassium currents in rat pyramidal neurons acutely isolated from hippocampal regions CA1 and CA3. *J Neurophysiol* **74**, 1982–1995.

Klemic KG, Kirsch GE & Jones SW (2001). U-type inactivation of Kv3.1 and Shaker potassium channels. *Biophys J* **81**, 814–826.

Klemic KG, Shieh CC, Kirsch GE & Jones SW (1998). Inactivation of Kv2.1 potassium channels. *Biophys J* **74**, 1779–1789.

Lien CC, Martina M, Schultz JH, Ehmke H & Jonas P (2002). Gating, modulation and subunit composition of voltage-gated K^+ channels in dendritic inhibitory interneurones of rat hippocampus. *J Physiol* **538**, 405–419.

Liss B, Franz O, Sewing S, Bruns R, Neuhoff H & Roeper J (2001). Tuning pacemaker frequency of individual dopaminergic neurons by Kv4.3L and KChip3.1 transcription. *EMBO J* **20**, 5715–5724.

Martina M, Schultz JH, Ehmke H, Monyer H & Jonas P (1998). Functional and molecular differences between voltage-gated K^+ channels of fast-spiking interneurons and pyramidal neurons of rat hippocampus. *J Neurosci* **18**, 8111–8125.

Mathie A, Clarke CE, Ranatunga KM & Veale EL (2003). What are the roles of the many different types of potassium channel expressed in cerebellar granule cells? *Cerebellum* **2**, 11–25.

Menegola M & Trimmer JS (2006). Unanticipated region- and cell-specific downregulation of individual KChIP auxiliary subunit isotypes in Kv4.2 knock-out mouse brain. *J Neurosci* **26**, 12137–12142.

Millar JA, Barratt L, Southan AP, Page KM, Fyffe RE, Robertson B & Mathie A (2000). A functional role for the two-pore domain potassium channel TASK-1 in cerebellar granule neurons. *Proc Natl Acad Sci U S A* **97**, 3614–3618.

Nadal MS, Amarillo Y, Vega-Saenz de Miera E & Rudy B (2001). Evidence for the presence of a novel Kv4-mediated A-type K^+ channel-modifying factor. *J Physiol* **537**, 801–809.

Nadal MS, Amarillo Y, Vega-Saenz de Miera E & Rudy B (2006). Differential characterization of three alternative spliced isoforms of DPPX. *Brain Res* **1094**, 1–12.

Nadal MS, Ozaita A, Amarillo Y, Vega-Saenz de Miera E, Ma Y, Mo W, Goldberg EM, Misumi Y, Ikehara Y, Neubert TA & Rudy B (2003). The CD26-related dipeptidyl aminopeptidase-like protein DPPX is a critical component of neuronal A-type K^+ channels. *Neuron* **37**, 449–461.

Patel SP & Campbell DL (2005). Transient outward potassium current, 'Ito', phenotypes in the mammalian left ventricle: underlying molecular, cellular and biophysical mechanisms. *J Physiol* **569**, 7–39.

Perney TM, Marshall J, Martin KA, Hockfield S & Kaczmarek LK (1992). Expression of the mRNAs for the Kv3.1 potassium channel gene in the adult and developing rat brain. *J Neurophysiol* **68**, 756–766.

Pioletti M, Findeisen F, Hura GL & Minor DL Jr (2006). Three-dimensional structure of the KChIP1-Kv4.3 T1 complex reveals a cross-shaped octamer. *Nat Struct Mol Biol* **13**, 987–995.

Ramakers GM & Storm JF (2002). A postsynaptic transient K^+ current modulated by arachidonic acid regulates synaptic integration and threshold for LTP induction in hippocampal pyramidal cells. *Proc Natl Acad Sci U S A* **99**, 10144–10149.

Ren X, Hayashi Y, Yoshimura N & Takimoto K (2005). Transmembrane interaction mediates complex formation between peptidase homologues and Kv4 channels. *Mol Cell Neurosci* **29**, 320–332.

Rhodes KJ, Carroll KI, Sung MA, Doliveira LC, Monaghan MM, Burke SL, Strassle BW, Buchwalder L, Menegola M, Cao J, An WF & Trimmer JS (2004). KChIPs and Kv4 α subunits as integral components of A-type potassium channels in mammalian brain. *J Neurosci* **24**, 7903–7915.

Riazanski V, Becker A, Chen J, Sochivko D, Lie A, Wiestler OD, Elger CE & Beck H (2001). Functional and molecular analysis of transient voltage-dependent K^+ currents in rat hippocampal granule cells. *J Physiol* **537**, 391–406.

Rudy B, Hoger JH, Lester HA & Davidson N (1988). At least two mRNA species contribute to the properties of rat brain A-type potassium channels expresed in *Xenopus* oocytes. *Neuron* **1**, 649–658.

Rudy B, Sen K, Vega-Saenz de Miera E, Lau D, Ried T & Ward DC (1991). Cloning of a human cDNA expressing a high voltage-activating, TEA-sensitive, type-A K^+ channel which maps to chromosome 1 band p21. *J Neurosci Res* **29**, 401–412.

Schoppa NE & Sigworth FJ (1998). Activation of Shaker potassium channels. III. An activation gating model for wild-type and V2 mutant channels. *J Gen Physiol* **111**, 313–342.

Schoppa NE & Westbrook GL (1999). Regulation of synaptic timing in the olfactory bulb by an A-type potassium current. *Nat Neurosci* **2**, 1106–1113.

Schroter KH, Ruppersberg JP, Wunder F, Rettig J, Stocker M & Pongs O (1991). Cloning and functional expression of a TEA-sensitive A-type potassium channel from rat brain. *FEBS Lett* **278**, 211–216.

Sekirnjak C, Martone ME, Weiser M, Deerinck T, Bueno E, Rudy B & Ellisman M (1997). Subcellular localization of the K^+ channel subunit Kv3.1b in selected rat CNS neurons. *Brain Res* **766**, 173–187.

Serodio P, Kentros C & Rudy B (1994). Identification of molecular components of A-type channels activating at subthreshold potentials. *J Neurophysiol* **72**, 1516–1529.

Serodio P & Rudy B (1998). Differential expression of Kv4 K^+ channel subunits mediating subthreshold transient K^+ (A-type) currents in rat brain. *J Neurophysiol* **79**, 1081–1091.

Serodio P, Vega-Saenz de Miera E & Rudy B (1996). Cloning of a novel component of A-type K^+ channels operating at subthreshold potentials with unique expression in heart and brain. *J Neurophysiol* **75**, 2174–2179.

Shahidullah M & Covarrubias M (2003). The link between ion permeation and inactivation gating of Kv4 potassium channels. *Biophys J* **84**, 928–941.

Smith-Maxwell CJ, Ledwell JL & Aldrich RW (1998). Uncharged S4 residues and cooperativity in voltage-dependent potassium channel activation. *J Gen Physiol* **111**, 421–439.

Strassle BW, Menegola M, Rhodes KJ & Trimmer JS (2005). Light and electron microscopic analysis of KChIP and Kv4 localization in rat cerebellar granule cells. *J Comp Neurol* **484**, 144–155.

Stuart GJ, Dodt HU & Sakmann B (1993). Patch-clamp recordings from the soma and dendrites of neurons in brain slices using infrared video microscopy. *Pflugers Arch* **423**, 511–518.

Thompson SM (2007). IA in play. *Neuron* **54**, 850–852.

Tseng-Crank JC, Tseng GN, Schwartz A & Tanouye MA (1990). Molecular cloning and functional expression of a potassium channel cDNA isolated from a rat cardiac library. *FEBS Lett* **268**, 63–68.

Vega-Saenz de Miera E, Moreno H, Fruhling D, Kentros C & Rudy B (1992). Cloning of ShIII (Shaw-like) cDNAs encoding a novel high-voltage-activating, TEA-sensitive, type-A K^+ channel. *Proc R Soc Lond B Biol Sci* **248**, 9–18.

Wang S, Bondarenko VE, Qu YJ, Bett GC, Morales MJ, Rasmusson RL & Strauss HC (2005). Time- and voltage-dependent components of Kv4.3 inactivation. *Biophys J* **89**, 3026–3041.

Wang G, Shahidullah M, Rocha CA, Strang C, Pfaffinger PJ & Covarrubias M (2005). Functionally active t1–t1 interfaces revealed by the accessibility of intracellular thiolate groups in Kv4 channels. *J Gen Physiol* **126**, 55–69.

Wang H, Yan Y, Liu Q, Huang Y, Shen Y, Chen L, Chen Y, Yang Q, Hao Q, Wang K & Chai J (2007). Structural basis for modulation of Kv4 K^+ channels by auxiliary KChIP subunits. *Nat Neurosci* **10**, 32–39.

Weiser M, Bueno E, Sekirnjak C, Martone ME, Baker H, Hillman D, Chen S, Thornhill W, Ellisman M & Rudy B (1995). The potassium channel subunit KV3.1b is localized to somatic and axonal membranes of specific populations of CNS neurons. *J Neurosci* **15**, 4298–4314.

Weiser M, Vega-Saenz de Miera E, Kentros C, Moreno H, Franzen L, Hillman D, Baker H & Rudy B (1994). Differential expression of Shaw-related K^+ channels in the rat central nervous system. *J Neurosci* **14**, 949–972.

Zagha E, Ozaita A, Chang SY, Nadal MS, Lin U, Saganich MJ, McCormack T, Akinsanya KO, Qi SY & Rudy B (2005). DPP10 modulates Kv4-mediated A-type potassium channels. *J Biol Chem* **280**, 18853–18861.

Zagotta WN, Hoshi T & Aldrich RW (1994). Shaker potassium channel gating. III: Evaluation of kinetic models for activation. *J Gen Physiol* **103**, 321–362.

Acknowledgements

We wish to thank Brian Clark and Eddie Zagha for their critical review of this manuscript. This work was supported by National Institutes of Health grants NS045217 and NS30989 and NSF grant IBN-0314645 to B.R., National Institutes of Health grant NS032337 and Research Enhancement Award (REA) from Thomas Jefferson University to M.C.; and NIH training grant T32 AA007463 to K.D.

Supplemental material

Online supplemental material for this paper can be accessed at:
http://jp.physoc.org/cgi/content/full/jphysiol.2007.150540/DC1
and
http://www.blackwell-synergy.com/doi/suppl/10.1113/jphysiol.2007.150540